Article

Demonstration of 256 QAM 10 Gbps Signal Transmission over 570 km Fiber-based NG Radio over Fiber System

Hasan k. Al Deen [1], Haider J. Abd [1,2]
[1] *Department of Electrical Engineering, College of Engineering, University of Babylon, Hillah, Babil, Iraq. hasan.hasan.engh442@student.uobabylon.edu.iq*
[2] *Department of Biomedical Engineering, College of Engineering and Technologies, Al-Mustaqbal University, Hillah, Babil, Iraq. haider.jabber@uomus.edu.iq*

***Abstract*— The rapid development of the Fifth Generation (5G) networks encourages researchers to improve the Radio over Fiber (RoF) technique to achieve data rates of 10 Gbps and beyond. That led to a significant increase in bandwidth and range while reducing latency and cost. This paper evaluates an Analog Radio over Fiber (ARoF) technique compatible with Next-Generation (NG) long-haul communication systems, aiming for simplicity and lower cost. Transmitting a 28 GHz, 256 Quadrature Amplitude Modulation (QAM) signal through Single-Mode Fiber (SMF) is possible by modulating it through two parallel Mach-Zehnder Modulators (MZM), allowing signal reception over long distances. The Error Vector Magnitude (EVM) appraises performance of the system. The simulation results indicate that the prototype can transfer data at 10 Gbps through the optical link up to 570 km with an EVM of 3.375% and received optical power of 4.015 dBm. The proposed system supports a high bit rate and maintains the EVM within 3GPP limits, making it superior to peer publications and highly appropriate for NG long-haul communication systems.**

***Index Terms*—** Analog Radio Over Fiber, Centralized Radio Access Networks, Error Vector Magnitude, Quadrature Amplitude Modulation.

I. INTRODUCTION

Technological innovation and industrial transformation accelerate information and communication technology advancements, focusing on NG communication systems. Considering 5G as a base, intelligent communication, such as smart connectivity, quicker communication, and holographic connectivity, is automatically influenced by this progress [1]. RoF-based Centralized Radio Access Networks (C-RAN) can be a powerful tool for reducing operating costs and shifting the overall cost from User Equipment (UE) to Base Station (BS); with its help, the signals can be sent over vast distances and through heavily crowded locations. Large-scale opportunities exist in this field for basic and applied research and development, focusing on boosting bit rates and lessening the impact of

  ISSN 2179-1074

impairments [2]. Due to rising demand and network density, the Radio Frequency (RF) spectrum in the high-frequency bands is teetering towards constant saturation. Wireless access flexibility and high capacity of optical fiber can be combined effectively with RoF systems' flexibility and good trade-off between data broadcast capacity, usability, and overall installation and maintenance expenses [3].

Generating millimeter waves (mmWaves) based on RoF is one of the spectrum options for 5G due to the vast quantity of accessible bandwidth. The 5G networks will require current spectrum and mmWave frequency bands to achieve high capacity with large antenna arrays that help ease the difficult propagation conditions by mmWave communications. The 5G spectrum comprises three frequency bands: low band (600-700 MHz), sub-6 GHz (3-5 GHz), and millimeter-wave band (24-100 GHz) [4].

Two types of RoF: Analog-Radio-over-Fiber (ARoF) and Digital-Radio-over-Fiber (DRoF). In the ARoF technique as shown in Fig.1, the RF signal modulates on an optical carrier with the benefit of great spectrum effectiveness, which is the most frequent technique employed in RoF systems. Although it encourages straightforward designs for distant radio devices because all required to get the analog waveform back is a photodetector, it is susceptible to nonlinearities in the components [5]. In the DRoF technique, the information signal is sent through the fiber as a stream of binary bits, which has the benefit of being resistant to nonlinearity [6]. Even so, because it calls for analog-to-digital converters in the distant radio unit, which drains much power at high sampling rates, DRoF is sometimes viewed as needing to be more appealing. Additionally, the demand for high-accuracy digital-to-analog and analog-to-digital conversions adds to the expense of DRoF [7].

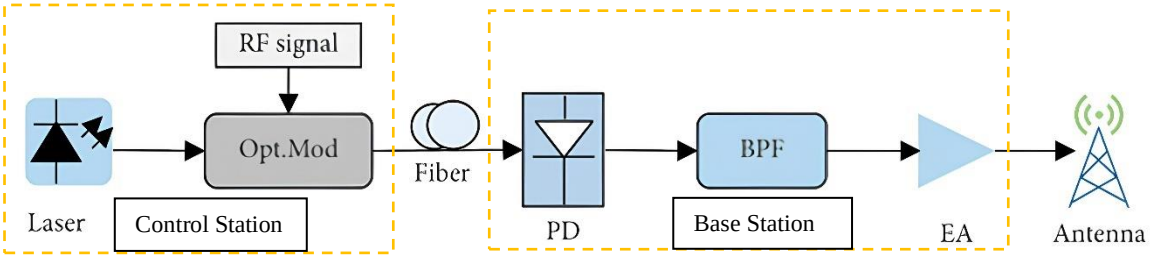

Fig. 1. General ARoF techniques. PD: photodetector, BPF: Band Pass Filter, EA: Electrical Amplifier, RF: Radio Frequency.

For short-haul systems, Multi-Mode Fiber (MMF) is preferable, while SMF is better suited for long-haul systems [8]. The optical receiver comprises electronics for data processing, a photodetector, and an amplifier. These components can significantly improve local or long-distance networks, while optical signals can still travel a considerable distance without amplifiers [9]. The Optical Band Pass Filter (OBPF) can exclude unwanted signals, significantly enhancing the system [10]. The Bit Error Rate (BER) and Quality Factor (Q) factor acquired from the Avalanche Photodiode (APD) diode are superior to those obtained from the PIN photodiode [11].

It is crucial to use advanced modulation techniques at high data rates and with high-frequency band

ISSN 2179-1074

while keeping costs low and maintaining simplicity to meet the requirements of 5G networks. Various techniques have been introduced and studied in the RoF architecture to improve system performance and overcome the nonlinear impairments that affect the ARoF link [12]. In the scholarly work detailed in reference [13], the authors analyzed three distinct optical modulation methods: Electro-Absorption Modulator (EAM), Directly Modulated Laser (DML), and the MZM or external modulator. Upon analyzing a 16 QAM signal, researchers discovered that the most effective system performance could be achieved by utilizing DML and MZM. However, the researchers provide a valuable insight into the integration of RoF and mmWave systems, a deeper exploration of nonlinear effects and their implications would enhance its practical relevance. To assess a greater degree of modulation, a team of researchers in [14] proposed utilizing a DML for facilitating the transmission of a 64-QAM at a frequency of 24 GHz across a 2-kilometer RoF system that incorporates both standard SMF-based infrastructure and free space transmission. The outcome of this approach was an EVM of 8.02 %. However, the DML is simple and cost-effective, but it is most suitable for low bit rates and short reach applications. An EVM of 3.14% can be achieved for a 256 QAM OFDM signal propagated over a 100-meter MMF at a wavelength of 850 nm with a carrier frequency of 3.5 GHz [15]. While the researcher employs the Digital Backward Propagation (DBP) and the Convolutional Neural Networks (CNNs) for nonlinear compensation. However, DBP's complexity prevents real-time implementation in practical systems additionally the CNNs models require continuous exposure to large volumes of data for training and learning. The authors in [16] investigated a RoF access network that generates mm-wave signals with frequencies of 20 GHz, 40 GHz, 60 GHz, and 80 GHz. The proposed RoF-DP-MZM system achieved excellent Bit Error Rate (BER) and Quality Factor (Q-factor) values for three encoding formats, demonstrating its effectiveness in creating 3-tupling mm-wave signals for multiple wireless accesses. However, conventional RoF systems still face limitations related to user capacity, sidebands, non-linearities, and system quality. While in [17], researchers achieved an EVM of 2.67% for a 3.5 Gbps 256 QAM signal modulated at 3.5 GHz over a 20-km SMF at 1310 nm. However, the use of 1310 nm Laser wavelength is suitable for shorter distances and offers some advantages, its limitations in terms of loss and dispersion make it less suitable for long-haul networks 1550 nm remains a preferred choice for extended-distance optical communication. In [18] the researchers propose a 60 GHz RoF system using coherent detection and optical heterodyning. It achieves impressive data transmission rates of 168 Gbps with 64-QAM. The system design includes Advanced Digital Signal Processing (ADSP) to mitigate impairments, enabling long-distance transmission over standard SMF. However, implementing coherent detection and optical heterodyning involves intricate components and algorithms, leading to potential cost and complexity challenges. Achieving high data rates often involves trade-offs with transmission distance. Balancing capacity and reach are essential for practical deployment.

However, RoF networks faces several technical challenges, as highlighted in references [13]-[18].

  ISSN 2179-1074

Among these challenges, a critical issue is mitigating the loss of signal due to the nonlinearity that exhibits the ARoF systems. There is a need to develop a new way to increase the distance between Control Station (CS) and BS while maintaining high data rates with mmWave signals to satisfy the NG communication system, which has led to the development of the proposed scheme.

The objective of this study is to analyze ARoF systems, considering their significance in NG wireless networks, particularly 5G C-RAN deployments. In this paper, we present a successful transmission experiment at a blazing 10 Gbps using ARoF technology, which is well-suited for the communication systems of the future operating within the C-band coverage. Our approach involves transmitting a 256 QAM signal over an optical fiber using a combination of parallel MZM and Dispersion Compensation Fiber (DCF). Remarkably, this setup achieves an impressive transmission distance of 570 km while maintaining excellent performance.

To optimize the system, we meticulously test and fine-tune various critical parameters. These include adjusting the Continuous Wave (CW) laser optical power, optimizing the MZMs' Extinction Ratio (ER), and precisely setting the phase shift angle. The result is an optimal EVM, ensuring reliable and efficient communication over long distances. Section II describes the proposed system's architecture, key components, and procedure principle of ARoF at high-frequency bands. The suggested model is compared with previous work, demonstrating its effectiveness and reliability performance. Section III analyzes and discusses the simulation results and system performance. Finally, conclusions are drawn in Section IV.

II. KEY COMPONENTS AND THE SYSTEM'S ARCHITECTURE.

The proposed ARoF system is designed, built, and evaluated using Optisystem software, as explained in Fig. 2. At the transmitter, the original signal is made with the 256 QAM symbol mapping. A pseudo-random binary sequence (PRBS) generator produces the bit stream in the QAM modulator building. This is accomplished through a serial to parallel conversion, which splits the bit sequence into two parallel subsequences. Each subsequence is then transferred on two quadrature carriers. The subsequences are up-sampling for In-phase (I) and quadrature (Q) signal signals using an M-ary Pulse Generator, additionally digitally upconverting the resultant NRZ bit streams of the I and Q channels to a carrier frequency (fc) of 28 GHz. The 256 QAM passband I and Q signals can express as [18]:

$$S(t) = I(t)sinw_c t + Q(t)cosw_c t \quad (1)$$

The electrical QAM signal will be evenly split into two output ports, with each port feeding parallel MZMs. The combined signal is then transmitted through the optical fiber to the BS.

ISSN 2179-1074

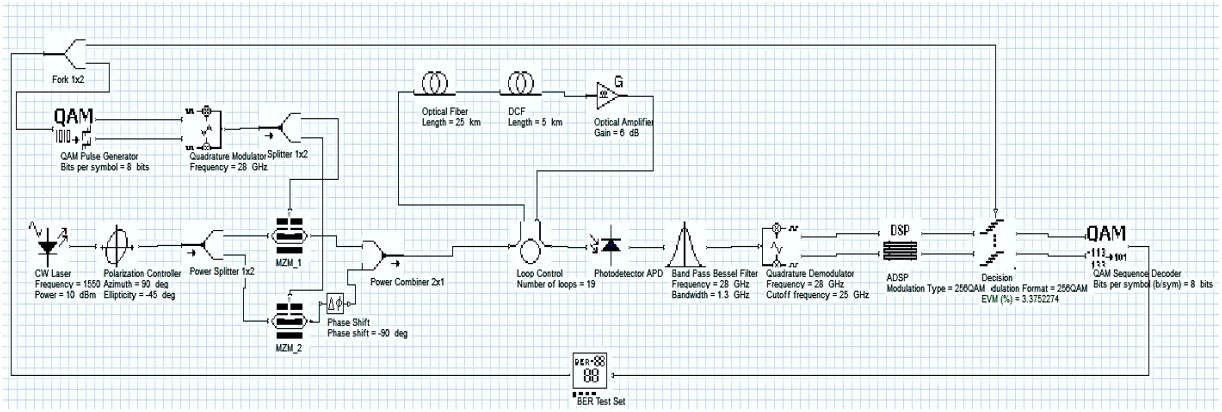

Fig. 2. Overall Proposed System Setup. DCF: Dispersion Compensating Fiber, CW: Continuous Wave, DSP: Digital Signal Processing, QAM: Quadrature Amplitude Modulation

The optical link utilizes a CW laser that emits light waves at 1550 nm with an average output power of 10 dBm and a linewidth of 0.1 MHz. A Polarization Controller (PC) is an optical device that enables adjustment of the polarization state of light by setting the input signal in any desired polarization state. A well-adjusted PC helps maximize signal quality, minimizing polarization-related impairments such as Polarization-Dependent Loss (PDL) and Polarization Mode Dispersion (PMD). It is significant to note that the polarization of the input signal does not affect the polarization of the output signal. In this work, the azimuth is set to 90 degrees, and the ellipticity is set to -45 degrees.

The output of a CW laser is split into two equal parts using a power splitter with a splitting ratio of (50:50). These two parts are then connected to Mach-Zehnder Modulators (MZM_1 and MZM_2). The output of MZM_2 is shifted by a phase of ($\pi/2$) before being combined with the output of MZM_1 using an optical power combiner. That means the two parallel MZMs modify the QAM signal with light waves produced by a laser source. We aim to find the optimal ER of the MZM for the best system performance. The output optical carrier of each one of the MZM_s is stated equation (2) [19]:

$$E_{1,2}(t) = E_{cw}\cos(\pi\, V(t)/2V_{\pi})\cos\,(w_{cw}t)) \tag{2}$$

Where E_{cw} and ω_{cw} are the amplitude and angular frequency of the input CW laser carrier, respectively, V_{π} is the half-wave voltage of the MZM and V(t) is the applied driving voltage. The loss of MZM is neglected. V(t) consisting of an electrical RF signal and a dc biased voltage is given by:

$$V(\mathrm{t}) = V_b + V_m\cos\,(w_{RF}t) \tag{3}$$

Where V_b is the dc biased voltage, V_m and w_{RF} are the modulation voltage and the angular frequency of electrical driving signal, respectively.

The output optical signal after the combiner can be modelled in first approximation with the following linearized model (neglecting the modulator chirp) [20].

$$E_{out}(t) = \frac{E_{cw}(t)}{2}(E_1(t) + E_2(t))\,exp(j\theta_o) \tag{4}$$

Where (θ_o) the phase angle that shifts the output of MZM_2 to get the optimal EVM result, in this work, it found $(-\frac{\pi}{2})$.

  ISSN 2179-1074

An SMF link transmits an optical signal to the BS. This SMF has an attenuation factor of 0.2 dB/km. However, this attenuation can lead to a phenomenon called Chromatic Dispersion (CD), which adversely affects the analog signal quality. To mitigate CD, a specialized fiber known as DCF is employed. DCF operates in the normal regime (where $\beta_2 > 0$) at the standard telecommunication wavelength of 1550 nm. Unlike standard SMF (which work in the anomalous regime), DCF has a negative chromatic dispersion factor ($D(\lambda)$) that effectively compensates for the dispersion induced by the SMF. Additionally, a flat gain optical amplifier (OP) (type Erbium-Doped Fiber Amplifiers (EDFAs)) is used to boost the optical power. The optical signal traverses through (N) Loop Control (utilized in the Optisystem program for long-distance channels; in this context, N is set to 19). Each loop comprises 25 km of standard SMF, 5 km of DCF, and an OP with a power output of 6 dBm. This meticulously crafted configuration guarantees dependable and efficient communication between the CS and the BS.

The optical modulated signal is fed to an extremely sensitive APD; this APD-PD converts the optical signal back into the electrical domain, which passes into the electrical filter with a bessel frequency transfer function centered at 28 GHz and a 1.3 GHz filter bandwidth that successfully removes utmost noise. A coherent amplitude demodulator for quadrature components (I and Q) implements an analog demodulator of 256 level. It employs a 28 GHz carrier generator for (I and Q) quadrature ingredients, which is the component that regenerates an electrical baseband signal. The ADSP component, as shown in Fig. 3, is a powerful tool used for digital domain impairment compensation. Its primary purpose is to aid in recovering the incoming transmission signal after coherent detection.

Transmission channel bandwidth noise is added to the optical signal, contaminating the received RF signal. The voltages added to the modulators generate an additional DC shift. It is compensated by the higher shaping factor, flatter phase delay, and flatter group delay of the DC blocking third-order Bessel filter. The output of the Bessel filter is sent through the resampling process and can be enhanced by the I Q compensation block. The resampling of (I and Q) signals has been conducted using a cubic interpolation method. The I Q compensation is used to mitigate amplitude and phase imbalances within the (I and Q) signal [18].

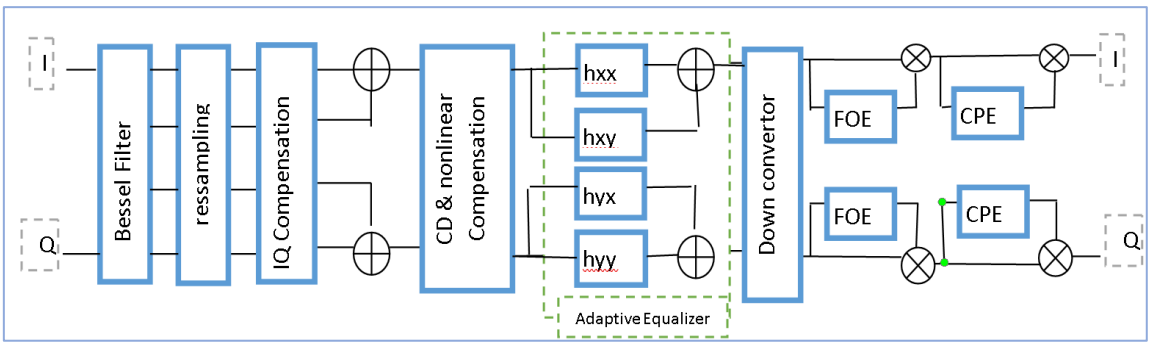

Fig. 3. The structure of the ADSP component, h (x, y): Signal's initial value tap weight, CPE: Carrier Phase Estimation, FOE: Frequency Offset Estimation

ISSN 2179-1074

Digital filtering used to compensate for CD. Nonlinear compensation is also performed using a DBP method. The adaptive equalizer is used to compensate for residual CD, Polarization Mode Dispersion (PMD) and to reduce inter-symbol interference. Down converter decimation filter used to reduce the sample rate. The mixing of received signal with the local oscillator frequency generated intermodulation product and deviates the frequency and phase components which leads to a symbol rotating constellation. Carrier Phase Estimation (CPE) used the blind phase search algorithm to recover accurate carrier phase and remove the remaining phase mismatch between the local oscillator and the signal [21]. While in Frequency Offset Estimation (FOE) it Estimates frequency offset due to local oscillator mismatches based on a feed forward spectral estimation method [22].

After receiving I and Q electrical signal channels from the ADSP stage, the decision component analyzes them, normalizes each I and Q channel's electrical amplitude to its corresponding 256 QAM level, and decides on each incoming symbol using the normalized threshold settings. The decision component executes a series of sequential functions, including DC blocking, decision-making, normalization, and EVM calculation. The I and Q components, supplied to the 256 QAM sequence decoder, reconstruct the bit sequence by utilizing two simultaneous input subsequences (I and Q quadrature carriers). Subsequently, this component generates an extensive bit sequence and transmits it to the BER test set, which is associated with the QAM pulse generator.

After transmitting a signal of 256 QAM centered at 28 GHz via an optical fiber of 570 km, the proposed ARoF system's functionality was evaluated, and the EVM was assessed. The EVM is a straightforward metric that measures the combined effect of all signal impairments in a system. It calculates the difference between the expected complex value of a demodulated symbol and the actual value of the received signal. The EVM limit for 5G signals modulated using 256 QAM modulation format has been established at 3.5 % by 3GPP [23]. In Equation 5, the Root Mean Square (RMS) values of EVM presented in this study are normalized to the average constellation power [24].

$$EVM\ \% = \sqrt{\frac{\frac{1}{M}\sum_{m=1}^{M}|S_m - S_{o,m}|^2}{\frac{1}{M}\sum_{m=1}^{M}|S_{o,m}|^2}} \tag{5}$$

Where $S_{0,\ m}$ is the ideal normalized constellation point of the M^{Th} symbol, S_m is the stream of measured symbols' normalized M^{Th} symbol, M is how many unique symbols there are in the constellation.

III. Simulation Results and Discussion

The performance of ARoF systems is assessed for the parameter setting as in Table I. The system is verified, and the EVM is calculated for different optical signal power, optical channel lengths, and ER of the MZM using the Optisystem software in design.

received 14 Nov 2023; for review 17 Jan 2024 accepted 25 Jun 2024

ISSN 2179-1074

TABLE I. SIMULATION PARAMETERS

Parameter	Value
Bit rates	10 Gbit/s
Carrier Frequency	28 GHz
MZM Extinction Ratio	10 dB
Laser wavelength	1550 nm
Modulation	256 QAM
APD-PD gain	5
Sample per bit	16
Fiber attenuation	0.2dB/ km

As depicted in Fig. 2, the RoF schematic diagram is designed and constructed in the following way. The transmitter generates a QAM signal with a radio frequency of 28 GHz and a data rate of 10 Gbps, then split into two equal parts. The optical carrier, developed from a CW laser of 1550 nm wavelength, is modulated with the electrical QAM signal using parallel MZM_s. The output of MZM_2 is further optically phase-shifted by -90 degrees. The outputs of the two MZM_s are merged using a power combiner to generate the optical modulated signal. The signal after the combiner is represented by Fig. 4, where Fig.4 (a) shows the optical spectrum and Fig.4 (b) depict the optical time domain waveform after the combiner.

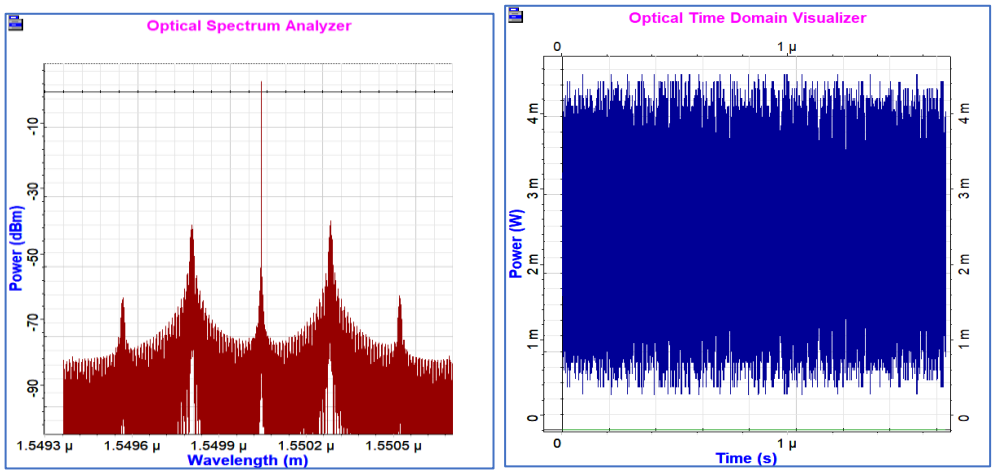

(a) (b)

Fig. 4. (a) Optical spectrum after combiner (b) optical time domain in electric domain signal

The optically modulated signal is transmitted over a 570 km optical link consisting of SMF and DCF to compensate for the dispersion that affects the system performance. An optical amplifier is used to enhance the optical power signal. The APD photodiode at BS receives the electric signal and converts it to electrical form, as shown in Fig. 5. The incoming signal undergoes bandpass filtering using a Bessel filter centered at 28 GHz. Subsequently, an amplitude demodulator, coherent for quadrature components (I and Q), recovers the QAM data at the same carrier frequency. However, the signal is significantly affected by noise, including E/O loss, optical fiber nonlinearity, and channel phase noise. To handle the baseband signal, the ADSP employs a range of techniques, starting with

ISSN 2179-1074

pre-processing and culminating in signal recovery.

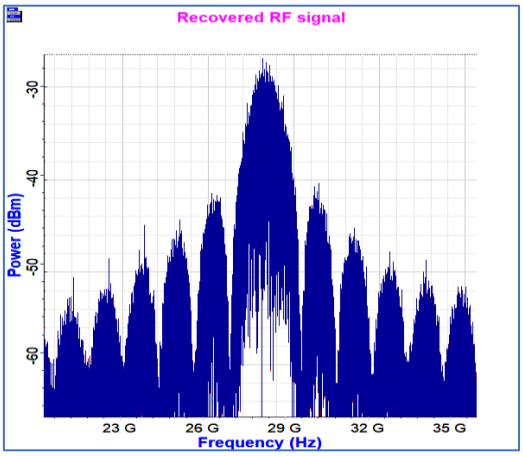

Fig. 5. Recovered electric signal.

In this section, we explore the received baseband signal before and after it passes through the ADSP block for 570 km fiber length. The signal is represented by Fig. 6, where Fig. 6 (a) shows the signal before the ADSP block, and Fig. 6 (b) shows the corresponding constellation diagram. As discussed in Section III, the phase misfit of the symbol path is caused by the optical and RF channel parameters. An ADSP block has been implemented using different methods and algorithms to mitigate this issue.

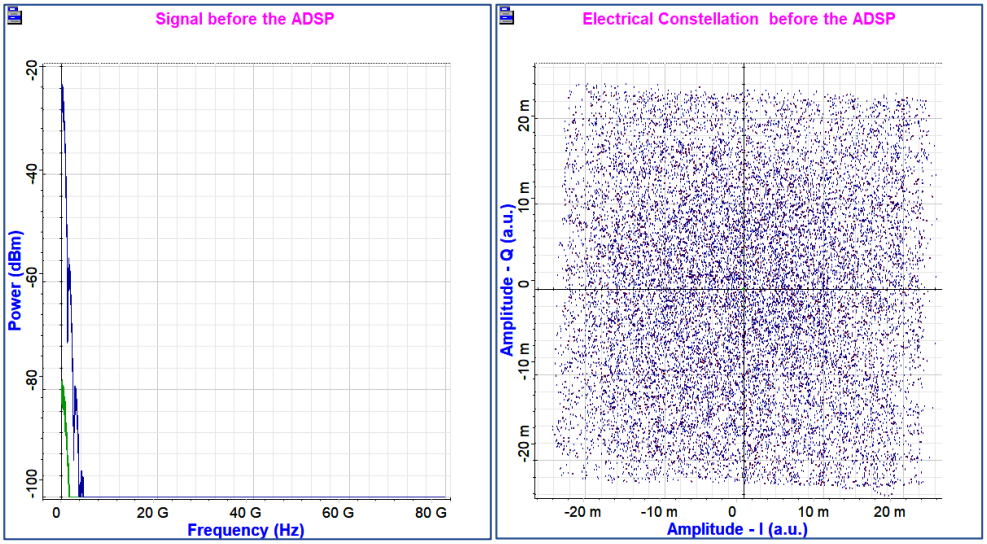

(a) (b)

Fig. 6. (a) The 256 QAM signal before the ADSP (b) constellation diagram before the ADSP

In Fig. 7 (a), the 256 QAM signal is displayed, and the corresponding constellation diagram is shown in Fig. 7 (b) next to the ADSP block. The demodulated signal is then processed in the decision component operations to measure the EVM of the received QAM symbol. The constellation diagram reveals a significant enhancement in the symbol path after passing through the ADSP block, which includes compensation for CD, (I and Q) imbalance, channel equalization, FOE, and CPE. After passing through the 256 QAM demodulator with an (8) Bits/symbol set, the post-received signal is transformed into a digital bit stream. After a 570 km fiber channel length, the received optical power

ISSN 2179-1074

is 4.015 dBm, and the EVM computation is 3.375%.

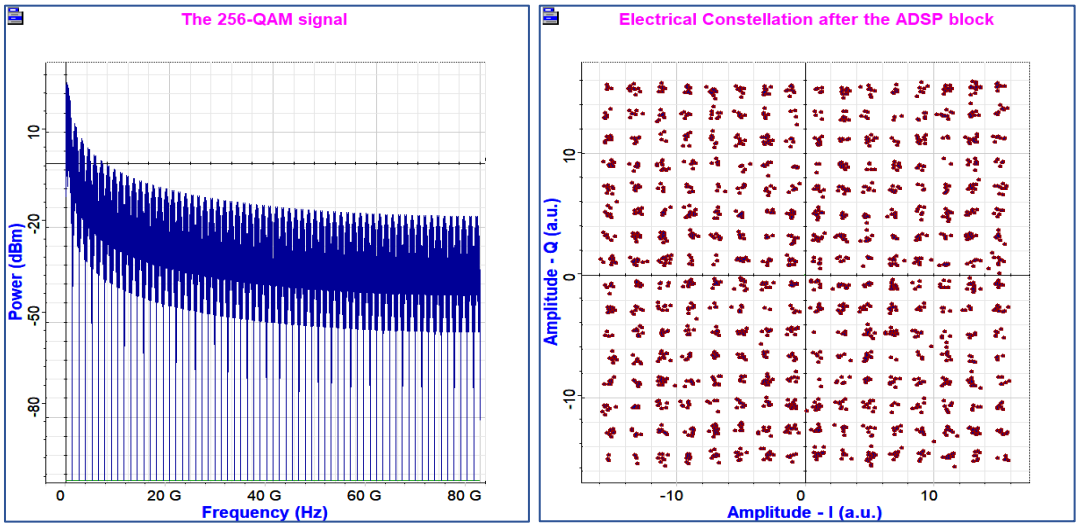

(a) (b)

Fig. 7. (a) The 256 QAM signal after the ADSP block (b) constellation diagram after the ADSP block

We varied the CW optical power and evaluated the EVM in each case to further test the proposed technique at different power levels. Fig. 8 (a) shows the EVM % vs. CW laser power plot with varying laser power from -5 dBm to 15 dBm at an optical channel length of 570 km. It indicates that the EVM values decrease linearly with increases in the laser power until reaching the 10 dBm laser power, which is the minimum value that meets the EVM limit for a 256 QAM signal. The EVM value increases with the rise of the CW laser power until it reaches 15 dBm.

In Fig. 8 (b), we plotted the relation between the EVM value for different fiber lengths. It demonstrates the EVM result after varying optical fiber lengths from 30 km to 600 km. We observed that the minimum EVM value can be achieved at 420 km, but as the fiber length increased, the EVM also increased and reached 3.375% after 570 km of optical medium length, which reaches the 3GPP limit of 3.5% for 256 QAM signals.

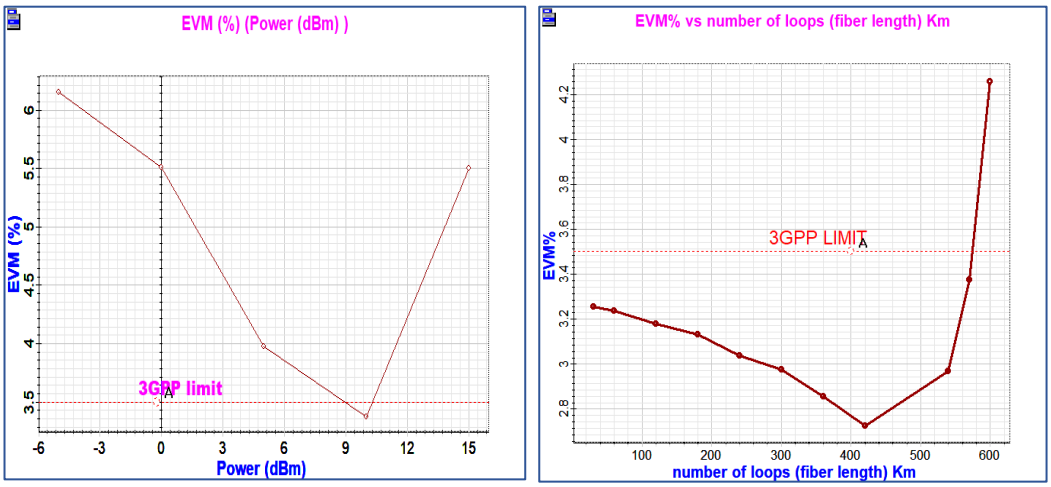

(a) (b)

Fig. 8. (a) The EVM % vs. CW laser optical power curve (b) The EVM % vs number of loops (fiber length)

ISSN 2179-1074

Fig. 9 depicts the relationship between EVM% and the ER of the MZM when varying the ER from -5 dBm to 15 dBm. The plot illustrates that the EVM value decreases as the ER increases. The optimal ER value is 10 dB, which complies with the 3GPP limit of the EVM. However, exceeding the ER value of 10 dB will lead to a decrease in the EVM value.

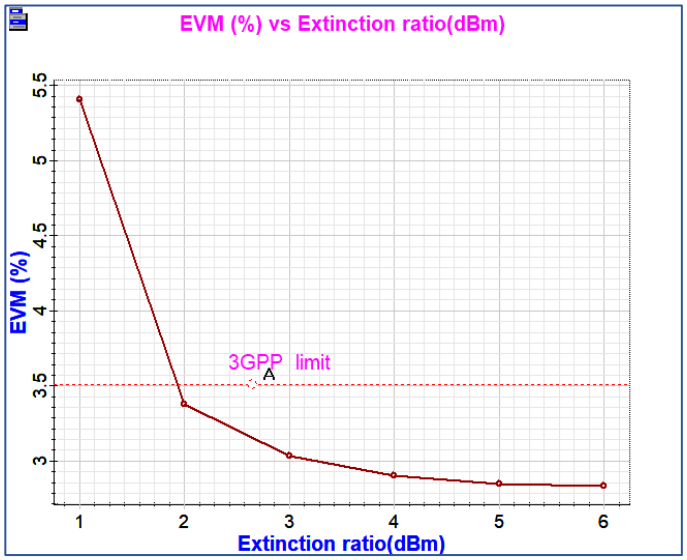

Fig. 9. The EVM % vs MZM Extinction ratio

Based on Fig. 8 and Fig. 9, it is evident that keeping the EVM within the 3GPP limit enables the transmission of C-band 256 QAM signals over an optical fiber link-based ARoF system, regardless of the optical power and the length of the fiber spans. Extensive measurements have demonstrated the suggested architecture's ability to support long-haul RoF networks for NG communication systems with lower transmitted power while delivering a high data rate that meets the 3GPP-EVM limit for 256 QAM. To ensure the effectiveness of the proposed method, another design was evaluated. Fig. 10 (a) shows that the signal was converted from electrical to optical form using a single MZM, eliminating the need for parallel MZMs. The optical signal propagated over 300 Km and exhibited effective reception, achieving an EVM of 3.195%. The constellation diagram of the received signal, post ADSP, is depicted in Fig. 10 (b).

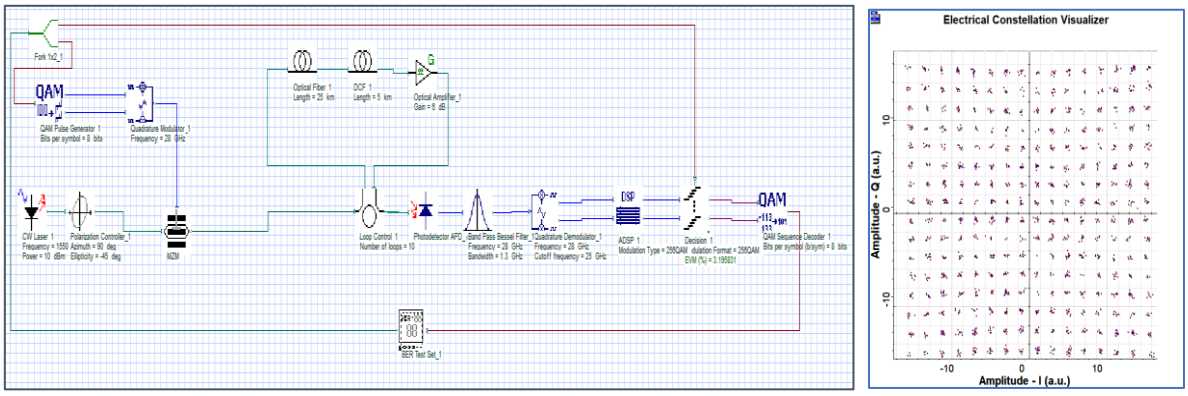

(a) (b)

Fig. 10. (a) Single MZM circuit design (b) corresponding constellation diagram after ADSP block

ISSN 2179-1074

In contrast to Fig. 11, the suggested approach used the Erbium-doped fiber amplifier (EDFA) instead of the DCF. The trial demonstrated that the 256 QAM signal can travel up to 10 km through optical fiber and 2m of EDFA with 3.396% EVM. However, this also highlights the importance of using DCF to counteract CD in optical fiber.

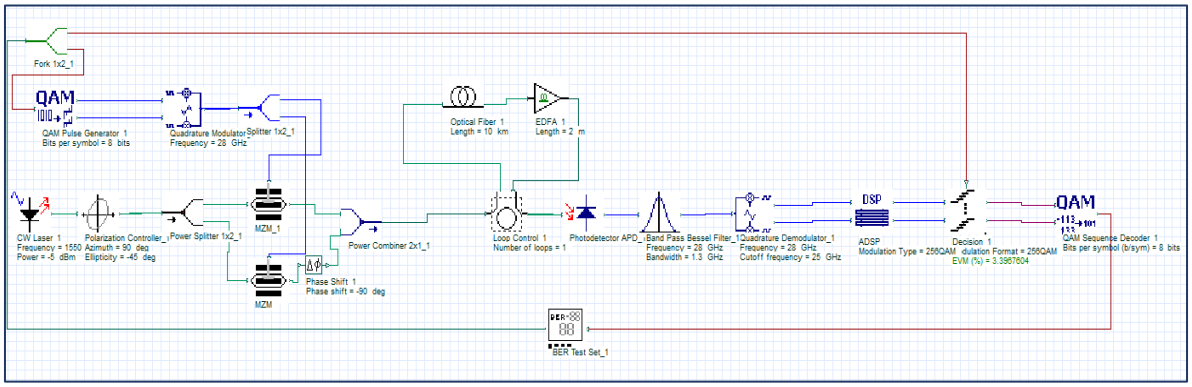

Fig. 11. System configuration used the Erbium-doped fiber amplifier (EDFA) in circuit design.

Table II presents a comparison between the proposed technique results and the findings from previous research. The comparison was conducted at different data rates, optically modulation types, and carrier frequencies. The proposed technique demonstrates superior performance compared with the direct modulation technique. However, its effectiveness is limited in long-distance transmissions, such as in [15] and [20]. It, where the signal was successfully received after 100m and 20 km, respectively. In [25],, which used external modulators with high data rates of 44.4 Gbps, the signal is received after 20 km. However, in [26], with the bit rate of 10 Gbps and the carrier frequency of 25 GHz, the fiber length conveys the signal is 90 km. When using the EAM modulation type as in [27] with at 100-GS/s and 27.5 GHz carrier frequency, it reaches a fiber distance of 10 km.

TABLE II. ACHIEVED RESULTS COMPARISON WITH RECENT WORK OF ROF, EVM: ERROR VECTOR MAGNITUDE.

Ref.	Modulation	Fiber length km	EVM %	Carrier frequency GHz	Optical modulation type	Data rate Gbps
proposed method	256 QAM	570	3.375	28	External	10
[15]	256 QAM	100 m	3.14	3.5	Direct	0.164
[17]	256 QAM	20	2.67	3.5	Direct	3.5
[25]	256 QAM	20	3.49	5	External	44.4
[26]	256 QAM	90	3.45	25	External	10
[27]	256 QAM	10	3.13	27.5	EAM	100-GS/s
[28]	256 QAM	42	3.4	26.2	External	88 GS/s

Based on Table II, the proposed system that utilized ADSP and DCF techniques along with a parallel MZM can support a high data rate over long distances while keeping the EVM within its standard limits. As a result, this method is highly effective for NG optical long-haul communication systems that operate under RoF technology.

ISSN 2179-1074

IV. CONCLUSION AND FUTURE WORK

The research study explored the transmission of mm Wave ARoF at high data rates using externally modulated parallel MZM. The EVM is used to appraise the system's performance. Results showed that a signal of 256 QAM in the 28 GHz frequency band was successfully transmitted over a fiber length of 570 km at 10 Gbps, with an EVM of 3.375% and a received optical power of 4.015 dBm. Several case studies were conducted, and it was found that using an EDFA instead of a DCF, the maximum transmission distance is 10 km with an EVM of 3.396%. Moreover, using a single MZM instead of parallel MZMs, the signal was successfully received after 300 km with an EVM of 3.195%. The proposed method demonstrated superior performance compared to similar studies in the literature and is well-suited for long-range NG communications. For future work it can be investigate more advanced modulation schemes beyond 256-QAM to achieve even higher data rates. As well as evaluate the system's performance in real-world scenarios, considering factors like environmental conditions and practical limitations.

REFERENCES

[1] P. Meena, M. B. Pal, P. K. Jain, and R. Pamula, "6G Communication Networks: Introduction, Vision, Challenges, and Future Directions," *Wireless Personal Communications*, vol. 125, no. 2, pp. 1097–1123, 2022, doi: 10.1007/s11277-022-09590-5.

[2] B. Kaur and N. Sharma, "Radio over Fiber (RoF) for Future Generation Networks," in *Broadband Connectivity in 5G and Beyond*, 2022, pp. 161–184. doi: 10.1007/978-3-031-06866-9_9.

[3] D. F. Paredes-Páliz, G. Royo, F. Aznar, C. Aldea, and S. Celma, "Radio over fiber: An Alternative Broadband Network Technology for IOT," *Electronics (Switzerland)*, vol. 9, no. 11, pp. 1–8, 2020, doi: 10.3390/electronics9111785.

[4] D. M. John, S. Vincent, S. Pathan, P. Kumar, and T. Ali, "Flexible Antennas for a Sub-6 GHz 5G Band: A Comprehensive Review," *Sensors*, vol. 22, no. 19. MDPI, 2022. doi: 10.3390/s22197615.

[5] X. Zeng *et al.*, "Constellation Independent Look-up Table Enabled Digital Predistortion for Digital-Analog Radio-over-Fiber System," in *2023 Optical Fiber Communications Conference and Exhibition (OFC)*, 2023, pp. 1–3. doi: 10.1364/OFC.2023.Tu2J.5.

[6] H. K. Al Deen and H. J. Abd, "Digitalized Radio over Fiber Network-Based Sigma Delta Modulation," *Fiber and Integrated Optics*, vol. 43, no. 3, pp. 97–110, 2024, doi: 10.1080/01468030.2024.2359919.

[7] L. Zhang *et al.*, "Toward Terabit Digital Radio Over Fiber Systems: Architecture and key Technologies," *IEEE Communications Magazine*, vol. 57, no. 4, pp. 131–137, 2019, doi: 10.1109/MCOM.2019.1800426.

[8] K. A. Abdulrahman and J. J. Hamad Ameen, "Interference Effect Evaluation with Radio over Fiber In 5G Mobile System," *Iraqi Journal of Computers*, vol. 23, no. 1, 2023, doi: 10.33103/uot.ijccce.23.1.7.

[9] U. U. Kazancili and N. Ö. Ünverdı, "Amplifier Analysis of Radio over Fiber Communication Systems," *Sigma Journal of Engineering and Natural Sciences*, vol. 37, no. 3, pp. 723–735, 2019.

[10] H. Termos, A. Mansour, and M. Ebrahim-Zadeh, "Establishment of an Electro-Optical Mixing Design on a Photonic SOA-MZI Using a Differential Modulation Arrangement," *Sensors*, vol. 23, no. 9, 2023, doi: 10.3390/s23094380.

[11] H. Hamadouche, B. Merabet, and M. Bouregaa, "Performance analysis of WDM PON Systems using PIN and APD Photodiodes," *International Journal of Computer Aided Engineering and Technology*, vol. 18, no. 1–3, pp. 1–18, 2023, doi: 10.1504/IJCAET.2023.127785.

[12] H. K. Al Deen and H. J. Abd, "An Investigation of Radio over Fiber (RoF) Communication System Technology: A Review," in *2022 2nd International Conference on Advances in Engineering Science and Technology (AEST)*, 2022, pp. 398–403. doi: 10.1109/AEST55805.2022.10413078.

[13] J. Bohata, M. Komanec, J. Spacil, R. Slavik, and S. Zvanovec, "Transmitters for Combined Radio over a Fiber and Outdoor Millimeter-Wave System at 25 GHz," *IEEE Photonics Journal*, vol. 12, no. 3, pp. 1–14, 2020, doi: 10.1109/JPHOT.2020.2997976.

[14] J. Bohata, M. Komanec, J. Spáčil, Z. Ghassemlooy, S. Zvánovec, and R. Slavík, "24–26 GHz Radio-over-Fiber and Free-Space Optics for Fifth-Generation Systems," *Optics Letters*, vol. 43, no. 5, pp. 1035–1038, 2018, doi: 10.1364/OL.43.001035.

[15] C. Y. Wu *et al.*, "Distributed Multi-User MIMO Transmission Using Real-Time Sigma-Delta-over-Fiber for Next Generation Fronthaul Interface," *Journal of Lightwave Technology*, vol. 38, no. 4, pp. 705–713, 2020, doi: 10.1109/JLT.2019.2947786.

  ISSN 2179-1074

[16] F. B. de Sousa, F. M. de Sousa, I. R. S. Miranda, W. Paschoal, and M. B. C. Costa, "Radio-Over-Fiber Dual-Parallel Mach–Zehnder Modulator System For Photonic Generation Of Millimeter-Wave Signals Through Two Stages," *Optical and Quantum Electronics*, vol. 53, no. 5, 2021, doi: 10.1007/s11082-021-02868-1.

[17] C. Y. Wu *et al.*, "Real-Time 4× 3.5 Gbps Sigma Delta Radio-over-Fiber for a Low-Cost 5G C-RAN Downlink," in *European Conference on Optical Communication (ECOC)*, Institute of Electrical and Electronics Engineers Incorporated, 2018, pp. 1–3. doi: 10.1109/ECOC.2018.8535235.

[18] D. Chack, S. Narayan Thool, and S. N. Thool, "High Capacity 64-Quadrature Amplitude Modulation Based Optical Coherent Transceiver for 60 GHz Radio over Fiber System," *Wireless Personal Communications*, vol.132, no.1, pp. 183–204, 2023, doi: 10.21203/rs.3.rs-586845/v1.

[19] S. Naing and M. Htet, "Generation of Optical Carrier Suppressed Signal for Radio-over-Fiber (RoF) System Using Dual-Drive Mach-Zehnder Modulator," *International Journal of Scientific and Research Publications*, vol. 4, no. 9, 2014, [Online]. Available: www.ijsrp.org

[20] H. Li et al., "Low Power All-Digital Radio-over-Fiber Transmission for 28-GHz Band using Parallel Electro-Absorption Modulators," *2020 Optical Fiber Communications Conference and Exhibition (OFC), San Diego, CA, USA*, 2020, pp. 1-3.

[21] Y. Li *et al.*, "Post-FEC Performance of Pilot-Aided Carrier Phase Estimation over Cycle Slip," *Applied Sciences (Switzerland)*, vol. 9, no. 13, pp. 230–235, 2019, doi: 10.3390/APP9132749.

[22] X. Zhang, C. Ju, D. Wang, Y. Zhao, P. Xie, and N. Liu, "Hardware-Efficient And Accurately Frequency Offset Compensation Based On Feedback Structure And Polar Coordinates Processing," *Optical and Quantum Electronics*, vol. 55, no. 2, p. 182, 2023, doi: 10.1007/s11082-022-04412-1.

[23] Y. Li and M. El-Hajjar, "Intelligent Analog Radio Over Fiber aided C-RAN for Mitigating Nonlinearity and Improving Robustness," in *Proceedings - IEEE Symposium on Computers and Communications*, Institute of Electrical and Electronics Engineers Incorporated, 2022, pp. 1–6. doi: 10.1109/ISCC55528.2022.9912819.

[24] M. U. Hadi, H. Jung, P. A. Traverso, and G. Tartarini, "Experimental Evaluation of Real-Time Sigma-Delta Radio over Fiber System for Fronthaul Applications," *International Journal of Microwave and Wireless Technologies*, vol. 13, no. 8, pp. 756–765, 2021, doi: 10.1017/S1759078720001282.

[25] Md. R. N. Babir and P. K. Choudhury, "On the Performance of High Order QAM Signals for Analog and Digital Radio over Fiber Systems," in *2017 4th International Conference on Advances in Electrical Engineering (ICAEE)*, 2017, pp. 379–382. doi: 10.1109/ICAEE.2017.8255385.

[26] O. Jothi, E. Ataro, and S. Musyoki, "Performance Evaluation of a SCM-OFDM Radio over Fiber System for the Mobile Fronthaul," *International Journal of Electrical and Electronic Engineering and Telecommunications*, vol. 11, no. 3, pp. 175–183, 2022, doi: 10.18178/ijeetc.11.3.175-183.

[27] H. Li *et al.*, "Real-Time 100-GS/s Sigma-Delta Modulator for All-Digital Radio-Over-Fiber Transmission," *Journal of Lightwave Technology*, vol. 38, no. 2, pp. 386–393, 2020, doi: 10.1109/JLT.2019.2931549.

[28] D. Che, "Digital SNR Adaptation of Analog Radio-over-Fiber Links Carrying up to 1048576-QAM Signals," in *2020 European Conference on Optical Communications (ECOC) 2020*, Institute of Electrical and Electronics Engineers Incorporated, 2020, pp. 1–4. doi: 10.1109/ECOC48923.2020.9333307.

received 14 Nov 2023; for review 17 Jan 2024 accepted 25 Jun 2024

ISSN 2179-1074